Observational Study

Medicine®

OPEN

Severe types of fetopathy are associated with changes in the serological proteome of diabetic mothers

Arthur T. Kopylov, MD, PhD[a,*], Olga Papysheva, MD[b], Iveta Gribova, MD[c], Anna L. Kaysheva, PhD[a], Galina Kotaysch, MD[c], Lubov Kharitonova, MD[d], Tatiana Mayatskaya, MD[d], Malik K. Nurbekov, PhD[e], Ekaterina Schipkova, BS[e], Olga Terekhina, PhD[e], Sergey G. Morozov, MD, PhD[c,e]

Abstract

Pregestational or gestational diabetes are the main risk factors for diabetic fetopathy. There are no generalized signs of fetopathy before the late gestational age due to insufficient sensitivity of currently employed instrumental methods. In this cross-sectional observational study, we investigated several types of severe diabetic fetopathy (cardiomyopathy, central nervous system defects, and hepatomegaly) established in type 2 diabetic mothers during 30 to 35 gestational weeks and confirmed upon delivery. We examined peripheral blood plasma and determined a small proportion of proteins strongly associated with a specific type of fetopathy or anatomical malfunction. Most of the examined markers participate in critical processes at different stages of embryogenesis and regulate various phases of morphogenesis. Alterations in CDCL5 had a significant impact on mRNA splicing and DNA repair. Patients with central nervous system defects were characterized by the greatest depletion (*ca*. 7% of the basal level) of DFP3, a neurotrophic factor needed for the proper specialization of oligodendrocytes. Dysregulation of noncanonical wingless-related integration site signaling pathway (Wnt) signaling guided by pigment epithelium-derived factor (PEDF) and disheveled-associated activator of morphogenesis 2 (DAAM2) was also profound. In addition, deficiency in retinoic acid and thyroxine transport was exhibited by the dramatic increase of transthyretin (TTHY). The molecular interplay between the identified serological markers leads to pathologies in fetal development on the background of a diabetic condition. These warning serological markers can be quantitatively examined, and their profile may reflect different severe types of diabetic fetopathy, producing a beneficial effect on the current standard care for pregnant women and infants.

Abbreviations: APOA1 = apolipoprotein A-I, Bcl-2 = apoptosis regulator Bcl-2, BMI = body mass index, C2 = complement factor C2, CDC5L = cell division cycle 5-like protein, CNSD = central nervous system depression, CRDM = cardiomyopathy, DAAM2 = disheveled-associated activator of morphogenesis 2, DF = diabetic fetopathy, DPF3 = zinc finger protein DPF3, FC = fold-change, FDR = false discovery rate, GDM = gestational diabetes mellitus, GO = gene ontology, HPMG = hepatomegaly, LAMB4 = laminin subunit β4, LRG1 = leucine-rich alpha-2-glycoprotein, LRP6 = low-density lipoprotein receptor-related protein 6, PCA = principal component analysis, PEDF = pigment epithelium-derived factor, PLRG1 = pleiotropic regulator 1, PPI = protein-protein interaction, PRP19α = pre-mRNA-processing factor 19, RBP = retinol binding protein, RNS = reactive nitrogen species, ROR2 = tyrosine-protein kinase transmembrane receptor ROR2, ROS = reactive oxygen species, RUNX = runt-related transcription factors, T2DM = type 2 diabetes mellitus, TGF-β = transforming growth factor beta, TSP1 = thrombospondin-1, TTHY = transthyretin, Wnt = wingless-related integration site signaling pathway.

Keywords: cardiomyopathy, central nervous system defects, diabetes mellitus, fetopathy, hepatomegaly, pregnancy

Editor: Daryle Wane.

This work was performed in the framework of Russian Federation Fundamental Research Programm for 2021–2030 years.

The authors have no conflicts of interests to disclose.

Supplemental Digital Content is available for this article.

All data generated or analyzed during this study are included in this published article [and its supplementary information files].

[a] *Institute of Biomedical Chemistry, 10 Pogodinskaya str., Moscow, Russia,* [b] *S.S. Yudin 7th State Clinical Hospital, 4 Kolomenskaya str., Moscow, Russia,* [c] *N.E. Bauman 29th State Clinical Hospital, 2 Hospitalnaya sq., Moscow, Russia,* [d] *N.I. Pirogov Medical University, 1 Ostrovityanova st., Moscow, Russia,* [e] *Institute of General Pathology and Pathophysiology, 8 Baltyiskaya str., Moscow, Russia.*

[*] *Correspondence: Arthur T. Kopylov, Department of Proteomic Research, Institute of Biomedical Chemistry, Biobanking, 10 Pogodinskaya str., Bld. 8, 119121 Moscow, Russia (e-mail: a.t.kopylov@gmail.com).*

How to cite this article: Kopylov AT, Papysheva O, Gribova I, Kaysheva AL, Kotaysch G, Kharitonova L, Mayatskaya T, Nurbekov MK, Schipkova E, Terekhina O, Morozov SG. Severe types of fetopathy are associated with changes in the serological proteome of diabetic mothers. Medicine 2021;100:45(e27829).

Received: 19 July 2021 / Received in final form: 27 October 2021 / Accepted: 29 October 2021

http://dx.doi.org/10.1097/MD.0000000000027829

1. Introduction

Diabetic fetopathy (DF) is a severe complication defined as systematic changes in newborns that can be caused by maternal pre-existing (type 1 or type 2 [T2DM]) or gestational diabetes mellitus (GDM). Due to the onset and duration of glucose intolerance during pregnancy, maternal hyperglycemia may stipulate diabetic embryopathy, resulting in congenital morphogenic or endocrine impairments, and spontaneous abortion.[1] DF can be found in early development by ultrasound examination and Doppler scanning during pregnancy. However, due to insufficient testing sensitivity, the diagnostics of DF usually occurs at late gestational age (beyond the 30th gestational week). A phenotypic analysis may have the highest diagnostic value to reveal the grade of fetal hepatomegaly, cardiomyopathy, and pancreatic enlargement, but the eventual results are reported upon delivery.[2,3]

The affected newborns may suffer metabolic syndrome, have a risk of obesity, and respiratory distress.[1,4] As a consequence of maternal diabetic status, the growing population of infants with metabolic syndrome raises great concern about cardiovascular disease developing as early as adolescence.[5] The most prevalent sign of DF is macrosomia, which results from maternal diabetes and can be considered a highly valuable predictor for later glucose intolerance and a high-risk factor for improper fetal development. Up to 45% of infants born from diabetic mothers have macrosomia, which is almost 3 times higher than the rate in normoglycemic patients.[6]

Adipose tissue, which produces adiponectin, tumor necrosis factor-alpha, interleukin-6, interleukin-10, and leptin, makes the main contribution to insulin sensitivity in pregnancy.[7,8] Maternal glycemic control is impaired, while the insulin resistance is being increased, so the level of circulating glucose is increased. The problem is that excessive maternal glucose may cross the placental barrier, whereas insulin may not. Starting in the second trimester, the fetal pancreas is already competent to secrete insulin. Therefore, the combined condition of maternal hyperglycemia and excessive secretion of insulin in the fetus raises the risk of increased fat production, leading to macrosomia and malfunctions in morphogenesis.[6]

Heart defects are the most common type of diabetic fetopathy, with a prevalence of up to 12%.[9] There is evidence that exactly maternal insulin resistance and high glucose levels are mainly responsible for the improper differentiation of cardiomyocytes and heart malformation.[10] Hypertrophic cardiomyopathy symptoms, in the form of asymmetric septal enlargement with a disproportionally hypertrophic septum, were routinely found in 12.1% of infants affected by maternal diabetes.[10,11]

Neural tube formation is also profoundly affected by the maternal diabetic condition, which directly influences the regulation of a variety of embryonic genes, particularly of genes involved in wingless-related integration site signaling pathway (Wnt)- and transforming growth factor-beta (TGF-β) signaling.[12] Recent studies have demonstrated that the etiology of neural tube defects encompasses elevated levels of superoxide dismutase, inhibition of the pentose phosphate pathway, and extended oxidative stress.[13,14]

Hepatomegaly is also a common potential injury in infants caused by maternal diabetes and is strongly associated with macrosomia.[15] A strong predictive value of glycated hemoglobin for hepatomegaly has been proposed, but this indicator cannot be used by itself.[16] Ultrasound examination is still the most confident and reliable instrumental method for detecting fetal hepatomegaly.[17]

In this study, we report a cross-sectional study of patients with T2DM who delivered affected newborns with different types of diabetic fetopathy. We performed a proteomic assay and evaluated the results in a control group of nondiabetic pregnant women and a group of patients with T2DM. Based on the obtained results, we performed a quantitative analysis of a small fraction of proteins and placed the most significantly altered markers in the reconstructed signaling pathways that underlie morphogenesis and cardiomyocyte differentiation, as well as markers that exhibit neurotrophic properties and activities in mRNA splicing and DNA repair. Our results suggest that most mechanisms identified here are generalized for all types of diabetic fetopathy. Even so, there are few specific markers capable of distinguishing the considered pathologies.

2. Methods

2.1. Population

In total, n = 187 pregnant women at a gestational age of 30 to 35 weeks participated in the study between October 2019–March 2020. Of them, n = 147 patients had a history of T2DM for 7.6 ± 3.2 years and insulin therapy of 6.5 ± 2.5 IU/day. Patients were stratified according to the type of diabetic fetopathy manifested in newborns upon delivery as follow: the group with cardiomyopathy (CRDM) comprised of n = 37 subjects with a body mass index (BMI) = 28.78 ± 4.42 kg/m^2 and age 25.4 ± 4.2 years; the group with malfunctions of the central nervous system (CNSD) comprised of n = 35 subjects with a BMI = 29.50 ± 3.21 kg/m^2 and age 25.9 ± 5.1 years; and the group with hepatomegaly (HPMG) consisted of n = 35 subjects with a BMI = 29.78 ± 3.55 kg/m^2 and age 24.7 ± 4.7 years (Table 1). Patients with T2DM who ruled out the DF for newborns were combined in a separate group consisting of n = 40 subjects with BMI = 29.69 ± 4.13 kg/m^2 and age 25.4 ± 3.9 years (Table 1). The proportion of patients with Caesarean delivery was almost evenly distributed among T2DM subgroups and ranged from 10% (HPMG subgroup) to 13% (CNSD subgroup), but their total rate was higher than that of the control group (45% vs 30%, $P = .007$, Table 1). Control group (n = 40, BMI = 23.89 ± 4.29 kg/m^2, age 25.6 ± 2.6 years; Table 1) comprised pregnancies who gave birth healthy newborns and had no previous history of T2DM or GDM according to the criteria of the International Association of the Diabetes and Pregnancy Study Groups (revision 2010)[18] and adapted criteria of the National Association of Obstetrician and Gynecologist (revision 2012).

2.2. Ethical consideration and consent for publication

The study design was approved by the local Ethical Committee of the Perinatal Center at N.E. Baumann 29th Hospital (Moscow; local protocol identifier BAU-EP2020-R035.B02 on October 20, 2019). All handlings and use of material were provided according to the World Medical Association Declaration of Helsinki on Ethical Principles for Medical Research Involving Human Subjects (revision 2013). This paper does not contain any personal data in any form. All subjects gave their signed written consent to participate in the study. Consent of participation and data personal data security was obtained according to the National Legislation of the Russian Federation "On Personal Data" No. 152 issued on July 27, 2006. All subjects who participated in the study were anonymized. The authors complied with ethical standards and privacy policy and did not disclose any

Table 1

Main anthropometric and clinical records for patients with T2DM and control group of patients. Patient with T2DM were subdivided into 3 groups according the signs of diabetic fetopathy attributed to the delivered newborns: CRDM – cardiomyopathy, CNSD – syndrome of central nervous system depression and HPMG – hepatomegaly. Patients with T2DM, who gave birth of newborns reported as healthy upon delivery and had no signs of diabetic fetopathy indicated by ultrasound examination during pregnancy course, were considered as the second control group.

Group	T2DM					
Type of fetal complication	CRDM, n (%)	CNSD, n (%)	HPMG, n (%)	Healthy, n (%)	Control (healthy)	*P* value
Size, n (%)	37 (25)	35 (24)	35 (24)	40 (27)	40	.889
Age, yr, mean ± SD	25.4 ± 4.2	25.9 ± 5.1	24.7 ± 4.7	25.4 ± 3.9	25.6 ± 2.6	.903
BMI, kg/m^2, mean ± SD*	28.78 ± 4.42 (*P* = .021)	29.50 ± 3.21 (*P* = .027)	29.78 ± 3.55 (*P* = 0.015)	29.69 ± 4.13 (*P* = .018)	23.89 ± 4.29	.273
Family history of diabetes, n (%)	10 (7)	8 (5)	8 (5)	11 (7)	-	-
Duration of diabetes, yr, mean ± SD	7.8 ± 3.5	7.5 ± 4.2	8.0 ± 3.3	7.2 ± 4.1	-	.739
Fasting glucose level, mmol/L, mean ± SD	7.8 ± 0.7 (*P* = .009)	8.1 ± 0.7 (*P* = .003)	7.6 ± 1.2 (*P* = .007)	8.3 ± 0.6 (*P* = .004)	3.5 ± 0.4	.029
Maternal weight gain, mean ± SD, kg	10.7 ± 3.5	11.4 ± 2.8	11.2 ± 2.3	9.7 ± 4.1	9.1 ± 5.2	.724
Gestational age at delivery, days, mean	272	275	272	274	270	.951
Caesar delivery, n (%)	15 (10)	19 (13)	14 (10)	18 (12)	12 (30)	-
Fetal weight, g, mean ± SD	3906 ± 212	3812 ± 229	3888 ± 197	3195 ± 231	3125 ± 132	.031
Apgar-1 score, median (range)	8 (7–9)	8 (6–8)	8 (7–9)	9 (6–9)	9 (7–9)	.885
Apgar-5 score, median (range)	9 (8–10)	9 (7–10)	9 (8–10)	9 (8–9)	9 (8–10)	.963
Diabetic fetopathy score, median (range)	4 (2–7)	3 (2–4)	3 (1–5)	-	-	.093
Hypoglycemia, n (%)	11 (7)	12 (8)	8 (5)	5 (3)	2 (5)	.086

* BMI was measured between 25 to 27 weeks of gestational age after results of OGTT were obtained to avoid possible inclusion of patients with the gestational diabetes mellitus in the control group.

personal data of participated subjects in the paper or the Supplemental Digital Content materials in any form.

2.3. Diagnostic criteria of fetopathy

2.3.1. Phenotypic signs. Newborns were examined upon delivery according to the following criteria: macrosomia if weight exceeded 4000 g; plentiful lanugo (soft auricles, soft bones of the skull, copious lubrication, undescended testes in the scrotum in boys); and neonatal hypoglycemia if capillary glucose was below 2.6 mmol/L.

2.3.2. Perinatal damage of central nervous system. Depression of the central nervous system was defined as the suppression of spontaneous motor activity, decreased passive and active muscle tone (decreased ability to straighten the body and while being held by the shoulders, decreased tone of the flexors and extensors of the neck when transferred to sitting position), pathological eye symptoms, inhibition of Kussmaul's, Babkin's, and palmar grasp reflexes.

2.3.3. Fetal cardiomyopathy. Cardiomyopathy was established by echocardiographic study with visualization of septal hypertrophy (left ventricular septal hypertrophy). The thickness of the interventricular septum was measured in M-mode in the basal third if it exceeded 1.8 to 4.5 mm for a 1.5 h–1-year-old infant.

2.3.4. Hepatomegaly. Signs were recognized by echocardiographic study. The size of the liver and the diameter of the liver were measured by transverse scanning of the body to determine the distance between the most distant points of the right and left lobes. Craniocaudal size and anteroposterior size were determined during longitudinal scanning at the mid-clavicular line.

2.4. Sample collection and handling

Sample preparation was performed according to the protocol described in.[19] Briefly, following overnight fasting, peripheral blood was collected into EDTA-2K$^+$ tubes. Plasma was obtained after centrifugation at 10°C and 2500 *g* for 10 minutes. Protein concentration was measured using a bicinchoninic acid protein assay kit. A total of 100 μg of each sample was used for processing and enzymatic digestion with trypsin. Briefly, proteins were reduced by buffered 10 mM tris (2-carboxyethyl) phosphine hydrochloride and alkylated by 0.2% 4-vinylpyridine solution in 30% isopropanol prior to digestion with trypsin at 1:100 (w/w) ratio. Complete details of the protocol are given in (Supplemental Digital Content [Appendix A, http://links.lww.com/MD2/A648]).

2.5. High-resolution LC-MS analysis

Instrumental analysis was conducted as described in.[19] Briefly, the analysis was performed on a high-resolution Orbitrap Fusion (Thermo Scientific, Waltham, MA, USA) mass spectrometer equipped with a nano-flow NSI ions source and integrated with an Ultimate 3000RSLC (Thermo Scientific, Waltham, MA, USA) liquid chromatography system. Briefly, peptides were loaded (2 μL, or 1 μg of 500 ng/μL concentration) separated on an Acclaim Pepmap (75 μm × 150 mm, 1.8 μm particle size, 60A pore size) column at a flow rate of 0.30 μL/min in a gradient of mobile phase A (water) and B (90% acetonitrile and 10% methanol) both supplied with 0.1% formic acid and 0.03% acetic acid. Ion detection was performed with a resolution of R = 60K in a range of 425 to 1250 *m/z* in a tandem mode. Each sample was analyzed in 3 technical replicates. Complete workflow and details are available in (Supplemental Digital Content [Appendix A, http://links.lww.com/MD2/A648]).

2.6. Statistical analysis, quantitative estimation, and functional annotation

Peak lists obtained from spectra were identified using an Open Mass Spectrometry Search Algorithm version 2.1.9. The search

was conducted using Search GUI version 2.3.17.[20] Protein identification was conducted against a concatenated target/decoy database of human proteins (UniProt Knowledgebase release December 2019). The decoy sequences were created by reversing the target sequences in Search GUI. The identification settings were as follows: trypsin as a specific protease, with a maximum of 1 missed cleavage, tolerance of ±5 ppm as MS1 level and tolerance of ±0.0025 Da as MS2 level tolerances; variable modifications: oxidation of methionine (+15.994915 u), deamination of asparagine (+0.984016 u), deamination of glutamine (+0.984016 u). Peptides and proteins were inferred from the spectrum identification results using Peptide Shaker version 1.16.15.[21] Peptide Spectrum Matches (PSMs), peptides and proteins were validated at a 1.0% false discovery rate (FDR) estimated using the decoy hit distribution.[22] Excluded from validation were proteins identified by site only, external contaminants, and reversed proteins.

Bias-correction to exclude outliers was performed by Mann–Whitney *U* test at $P < .05$. Proteins shared between analyzed groups were normalized and ranged according to their normalized spectra abundancy factor (normalized spectra abundancy factor) representation for quantitative analysis. Alterations between groups were represented for proteins in *log*-fold changes with significance cut-off $P < .01$ (Kruskal–Wallis test) and were obtained by defining a linear model for each protein. A two-sample moderated *t*-test was used, and the reported *P* values were corrected for false discovery rate. To extract proteins specific for each subgroup, we used principal component analysis (PCA) classification analysis, and the differences between scores were compared by the Kruskal–Wallis test at $P < .01$.

To unveil biological processes and functions associated with meaningful alterations, proteins were submitted in Gene Ontology supported by the overrepresentation test (annotation release 20200407). Significance was estimated using Fisher exact test ($P < .001$) against the proteins identified in the control group, and Bonferroni correction was applied for adjusting the FDR-based *P* values.[23] Initial (raw) molecular pathways were extracted from the Kyoto Encyclopedia of Genes and Genomes[24] and the Reactome (version 72).[25]

3. Results

3.1. General clinical characteristics

Patients with T2DM did not differ significantly from the controls in BMI or fasting glucose level (Table 1). Maternal weight gain was marginally higher ($P = .724$) in patients with T2DM than in the control group (Table 1). Still, the subset of T2DM patients who delivered healthy newborns had baseline characteristics comparable to those of the control group in this indicator ($P = .694$, Table 1). Although patients with T2DM gave birth to newborns with different types of diabetic fetopathy predetermined by sonography examination, the Apgar-1 and Apgar-5 scores reported upon delivery were somewhat comparable to the scores reported in the control group (Table 1). The integrative score of diabetic fetopathy was distinctive between the CRDM, CNSD, and HPMG groups, but median values were indistinguishable across the study groups with antenatal complications (Table 1).

3.2. Identification of proteins characterizing the condition of antenatal complications

In total, we identified 378, of which 296 were shared by all the study groups. Using the Mann–Whitney *U* test with raw $P < .05$ and fold-change >1.5 or <0.8 as the cutoffs, only 42 proteins were determined to be significantly altered, and 30 proteins might have meaningful value to discriminate T2DM subgroups (healthy and different types of fetopathy under consideration, Table 1 and (Supplemental Digital Content [Appendix B, http://links.lww.com/MD2/A649]). The significant proteins with $P < .05$ were input into PCA, with PC1 explaining 18% of the variance and PC2 explaining 11%. PCA score discrimination analysis showed satisfactory segregation of T2DM patients who gave birth to healthy newborns from the control group, and good separation and dispersion of subgroups bearing signs of diabetic fetopathy from the control group and T2DM patients with healthy newborns (Fig. 1A). This indicates a meaningful impact of the diabetic status during gestation on the risk and complications of fetal morphogenesis.

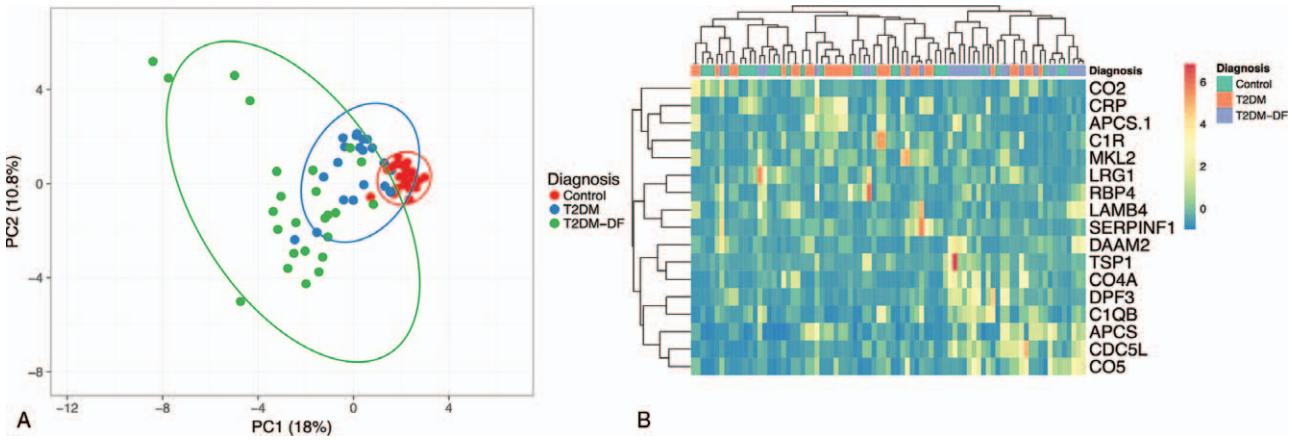

Figure 1. PCA score plot visualization using the 42 identified metabolites with the Mann–Whitney *U* test with raw *P* values less than 0.05 among patients in the control group (red), patients with T2DM who delivered healthy newborns (blue) and patients with T2DM who delivered newborns with different signs of diabetic fetopathy (CRDM, CNSD, and HPMG) (A). Heatmap of the significantly differentially expressed proteins identified in the study groups and discriminating the 3 types of fetopathy under consideration. The selected proteins had the smallest Mann–Whitney *U* test *P* values. Euclidean distance metrics and correlation clustering methods were applied for the hierarchical clustering of samples and identified proteins (B).

Table 2

The most significantly altered proteins segregate types of diabetic fetopathy from the control group and T2DM patients who gave birth of healthy newborns. Fold-change as the median measures is represented in a logarithmic (log_2) scale. The adjusted *P* value reported after Bonferroni correction for multiple testing. Significant fold-changes are color filled in the table.

Recommended protein name (according to the UniProt nomenclature)	Primary gene name	FC Log (2)			*P* value
		CNSD	HPMG	CRDM	
Pigment epithelium-derived factor	SERPINF1	1.103	0.600	0.314	<.001
Thrombospondin-1	TSP1	1.394	0.558	0.471	.004
Zinc finger protein DPF3	DPF3	−3.833	0.051	1.033	.005
Complement C4-A	CO4A	0.539	−0.131	0.044	.002
Complement C1q subcomponent subunit C	C1QC	0.543	0.483	0.043	.003
Transthyretin	TTR	0.655	0.398	0.471	.006
Complement C1q subcomponent subunit B	C1QB	0.674	0.118	−0.437	.003
Actin, cytoplasmic 1	ACTB	0.744	−0.103	−0.634	<.001
Cell division cycle 5-like protein	CDC5L	1.254	−0.068	0.198	.003
Complement C5	CO5	1.403	0.499	0.393	.004
Serum amyloid P-component	APCS	0.943	−0.418	0.269	<.001
Disheveled-associated activator of morphogenesis 2	DAAM2	0.145	0.734	1.068	.004
Laminin subunit beta-4	LAMB4	0.320	−1.085	1.664	.002
Neutrophil defensin 1	DEF1 *	−0.480	−1.058	−0.197	.006
Platelet basic protein	CXCL7 *	0.201	0.775	0.046	.006
N-acetylmuramoyl-L-alanine amidase	PGLYRP2 *	0.296	1.023	0.428	.004
Complement C1r subcomponent	C1R	-0.607	0.107	0.542	.005
Complement C2	CO2	−0.147	0.127	0.936	<.001
Leucine-rich alpha-2-glycoprotein	LRG1	0.369	−0.004	0.724	<.001
MKL/myocardin-like protein 2	MKL2	-0.073	0.372	0.798	.006

* $P < .01$ (Fisher exact test).

At the same time, it was established that only 20 out of 42 proteins could be considered significant (with $P < .01$) for distinguishing groups with antenatal pathologies (CRDM, CNSD, and HPMG) from groups of T2DM patients who gave birth to healthy newborns and the control group. This indicates different contributions of the selected proteins to antenatal complications. Meaningfully altered proteins (totally 17 proteins) were those that passed the Kruskal–Wallis test with a fold-change (FC) of FC>2 or FC < 0.5 (linear scale) at a $P < .01$. These proteins were selected for clustering into a heatmap and exhibited different patterns between the studied groups regarding antenatal pathologies (Fig. 1B and Table 2).

Some proteins among the selected were shared between 2 types of fetopathy under consideration and showed significant changes (for example, PEDF [pigment epithelium-derived factor] and thrombospondin-1 (TSP1) in the CNDS and HPMG groups; or DAAM2 (disheveled-associated activator of morphogenesis 2) and laminin subunit β4 (LAMB4) in the HPMG and CRDM groups, Table 2), whereas most of the determining markers demonstrated specificity to one specific type of antenatal complication and did not show relevance to other groups. Such segregation can probably be explained by the different mechanisms underlying CRDM, HPMG, and CNSD (Supplemental Digital Content [Appendix C, http://links.lww.com/MD2/A650]).

3.3. Functional categorization of the identified proteins

Most of the listed proteins (Table 2 and Supplemental Digital Content [Appendix B, http://links.lww.com/MD2/A649]) were related to biological processes regulating responses to stimuli (GO: 0048583, FDR = 6.19e-05) and stress (GO: 0080134, FDR = 0.00034), with an average local clustering coefficient of 0.575 (protein-protein interactions [PPI] enrichment $P < 1.0e-16$). Biological gene ontology (GO) terms stratification showed that upregulated proteins were related to defense responses (GO: 0006952, FDR = 3.54e-07), regulation of inflammatory responses (GO: 0050727, FDR = 1.03e-05), and responses to glucose (GO: 0009749, FDR = 0.0025). As expected, an overwhelming majority of the detected proteins (25 of 30 proteins; see Supplemental Digital Content [Appendix B, http://links.lww.com/MD2/A649 and C, http://links.lww.com/MD2/A650]), and Table 2) are localized in the extracellular space (GO: 0005576, FDR = 2.57e-13) and secretory granule lumen (GO: 0034774, FDR = 2.41e-07). Most of the proteins are characterized by the peptidase regulatory activity (GO: 0061134, FDR = 0.0037), oxygen binding and carry activities (GO: 0005344, FDR = 0.0074), and general activity guiding and regulating molecular function (GO: 0098772, FDR = 0.0282). Analysis of biochemical reactions and transformations revealed mutual signaling pathways such as in the innate immune response (HSA-168249, FDR = 5.52e-06), hemostasis (HSA-109582, FDR = 0.0015), and amyloid fiber formation (HSA-977225, FDR = 0.00029).

We next assembled the detected proteins into a molecular network that would reveal differences between examined types of diabetic fetopathy (CRDM, CNSD, and HPMG) and can determine triggers that selectively underline findings of fetopathy from patients with T2DM.

3.4. Protein-protein interactions

The PPI analysis was conducted on n = 30 proteins capable of discriminating T2DM patients from subjects with uncomplicated pregnancies (Supplemental Digital Content [Appendix C, http://links.lww.com/MD2/A650]). The assayed set completely covered the n = 17 most significant markers that segregated subgroups of patients with T2DM who delivered newborns with different types of diabetic fetopathy (CNSD, CRDM, and HPMG, Table 2).

There were nine markers shared in common between the 3 groups of diabetic fetopathy: apolipoprotein C-IV, galectin-3-binding protein, PEDF, TSP1, phosphatidylinositol-glycan-specific phospholipase D, insulin-like growth factor-binding protein complex acid-labile subunit, DPF3 (zinc finger protein DPF3), DAAM2 and LAMB4. The PPI analysis showed that these proteins produce a non-dense core of functional interactions (the coefficient of protein interactions is PPI = 0.389), except for a pair of PEDF and TSP1 and a cluster of DAAM2, DFP3, and LAMB4. Assumingly, it indicates the involvement of these proteins in the general processes leading to the development and progression of a particular fetopathy. Given a large number of group-specific markers, the common feature between studied pathologies most likely is a reflection of secondary signs of fetopathy and encompasses peripheral biological processes. The multiple molecular functions of the overlapping markers also support this proposition; these proteins are characterized by pleiotropic properties in the cell life cycle.

Three functional clusters (Supplemental Digital Content [Appendix C, http://links.lww.com/MD2/A650]) were formed by proteins involved in the immune response, proteins involved in the structuring of the intercellular space, and regulatory signaling proteins. Regulatory function is accomplished through the expression of proteolytic activity and the transmission of a signal (ligands) to receptors in signaling pathways, thereby forming a network of humoral regulation of the immune response and the protective response (GO: 0006952, $P = .00025$). The vast majority of the proteins participating in the interactions (17 proteins) were secreted proteins or proteins whose main activity was manifested in the extracellular space region (GO: 0044421, $P = 7.90e\text{-}09$), which indicates their high paracrine and endocrine potentials.

4. Discussion

4.1. The impact of mRNA splicing and DNA repair during embryogenesis

We focused on the most important markers, either cross-specific for several types of fetopathy or highly specific for a certain type, such as CDC5L (cell division cycle 5-like protein; Table 2), which is characterized by a low tissue specificity, but its highest expression is seen in the brain cortex, cerebellum, hippocampus, and thalamus. CDC5L exhibits a local core of interactions with actin, cytoplasmic 1, neutrophil defensin 1, and C2 (complement factor C2), with a local clustering coefficient of 0.782; the last 2 elements (neutrophil defensin 1 and C2) were not CNSD-specific (Table 2).

It is difficult to overestimate the role of CDC5L in the regulation of cell division, DNA repair, and activity, guiding mRNA splicing and maturation. Recent data highlighted the association of CDC5L with neuronal differentiation during embryogenesis, which depends on the assembly of an active complex (CDC5L/ adapter protein 14-3-3-beta/ pre-mRNA-processing factor 19 [PRP19α]) carrying necessary competencies for the differentiation of neurons.[26] Phosphorylation of the PRP19α by the protein kinase B is a critical step in complex assembly, whereupon it acquires a conformational ability to bind with adapter protein 14-3-3-beta for translocation into the nucleus (Fig. 2) and to meet CDC5L. Dysregulation of one of these elements leads to an adverse influence on neuronal differentiation and corrupts cell division since the complex regulates the G2/M phase.

The relationship between CDC5L and some neurodegenerative and neuroimmune diseases has been established in many studies, most of which findings were based on transcriptome analysis.[27–29] Adverse regulation of mRNA splicing in the cerebral cortex through, inter alia, malfunction of CDC5L leads to a decrease in proliferative activity and disruption of neuronal differentiation.[30] Comparable results were obtained in HeLa cell culture after immunoprecipitation of a complex of CDC5L with a pleiotropic regulator-1 (PLRG1) and heteronuclear ribonucleoprotein that was necessary for the activity of the mRNA splicing complex (Fig. 2). CDC5-mutant cells ($CDC5^{-/-}$) displayed an inability to build the complex, disruption of the splicing process, and extensive apoptosis.[31]

Evidence exists that translational repression and mRNA degradation are accomplished by circulating miRNAs tightly associated in different complexes.[32] A recent genome-wide associated study (GWAS) demonstrated that approximately 600 different miRNAs are expressed in the placenta and play a key regulatory role in embryogenesis and metabolic adaptation during fetal growth. Such molecules are released into the maternal circulation and may warn of placental dysfunction and the onset of GDM.[33] Our proteomic data suggest that an increased concentration of CDC5L (Table 2) may reflect malfunction mRNA splicing caused by dysregulation of placental miRNAs that influence mRNA processing.

DNA repair is another critical aspect of CDC5L activity. Embryonic fibroblast cells undergo active apoptosis through a p53-mediated mechanism in animals deficient in PLRG1.[34] The fundamental mechanism is a decreased ability of PLRG1 to assemble with CDC5L and consequent abolishment of the DNA repair mechanism (Fig. 2). As has been highlighted, such embryos demonstrated failed cell division and fragmented nuclei and died rather early due to apoptosis and re-localization of CDC5L from the nucleus to the cytoplasm (Supplemental Digital Content [Appendix C, http://links.lww.com/MD2/A650]). Repeated experiments on cultivating cardiomyocytes and neurons showed similar results where, apart from the re-localization of CDC5L, a decrease in the apoptosis regulator (Bcl-2) was noted.[34,35] Mice heterozygous for CDC5L had a survival rate not exceeding 25%. The surviving embryos were characterized by a dramatic increase in degraded neurons and cardiomyocytes (Supplemental Digital Content [Appendix C, http://links.lww.com/MD2/A650]), accompanied by reduced Bcl-2 and increased levels of phosphorylated transcription factor p53 but unaltered Bcl-2-associated X protein.[34]

Hence, CDC5L is an essential regulator of mRNA splicing and DNA repair in differentiating neurons during embryogenesis. Therefore, the drastically increased CDC5L in the CNSD group (Table 2) may suggest dysregulation of placental miRNA and the ongoing accumulation of DNA errors caused by the oxidative stress that is typical of patients with T2DM.

4.2. Extended activation of the immune response

Due to the many changes in homeostasis and immune response, elements of the complement system are typically considered nonspecific markers, although some of them were meaningful in both the CNSD (complement factors C1QC, C5, C4, C1QB) and CRDM groups (complement factors C1B, C2) (Table 2). As outlined above, in patients with T2DM, activation of the complement system is associated with oxidative stress caused by a

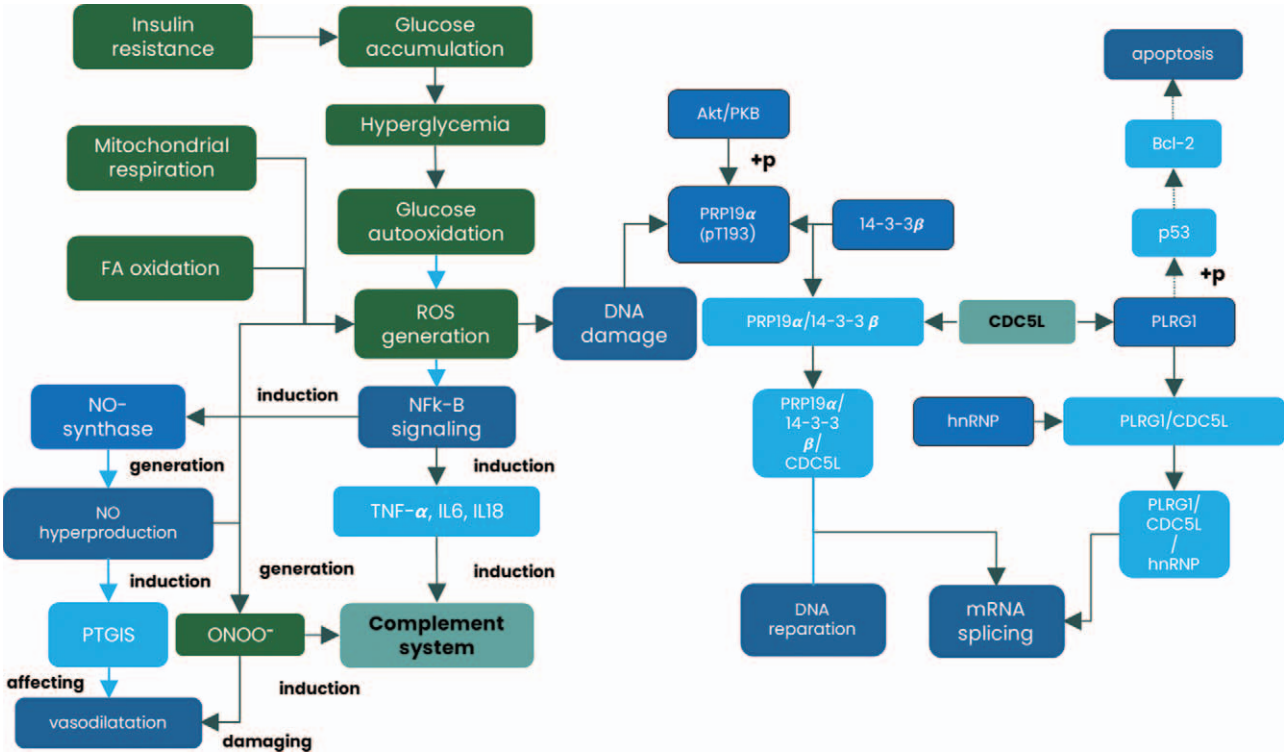

Figure 2. The proposed interplay between oxidative stress and impairments of DNA repair and RNA splicing in differentiating neurons and cardiomyocytes during embryogenesis in patients with T2DM. The development of insulin resistance leads to the accumulation of glucose in the blood, which undergoes auto-oxidation after a short time and makes a significant contribution to the generation of ROS along with fatty acid oxidation and mitochondrial respiration. Hyperproduction of ROS upregulates NF-κB signaling and increases the levels of tumor necrosis factor alpha, IL6, IL18, etc, activating the complement system. At the same time, NF-κB triggers NOS, generating NO (nitric oxide). When overproduced, NO quickly reacts with ROS and forms peroxynitrite, damaging the endothelium (diabetic angiopathy) and DNA and enhancing the response of the compliment system. The ongoing overproduction of ROS and RNS damages DNA and suppresses proper mRNA splicing in differentiating cells during embryogenesis, which triggers the implementation of CDC5L in DNA repair and mRNA splicing. Following phosphorylation by Akt kinase, PRP19α joins a heterodimeric complex with 14-3-3β and then CDC5L, which is capable of participating in mRNA splicing or DNA repair. On the other hand, complexation of CDC5L with PLRG1 allows assembly with hnRNP, which is also involved in splicing processes. Otherwise, there is an accumulation of DNA and splicing errors, disruption of protein synthesis, and disruption of cell division, leading to p53-dependent apoptosis and inhibition of the antiapoptotic factor Bcl-2.

hyperglycemic state.[36] Overproduction of reactive oxygen species (ROS) is aggravated by accumulated blood glucose undergoing auto-oxidation (Fig. 2), which activates the synthesis of prostaglandins and stimulates inflammatory reactions. A significant contribution is caused by activation of fatty acid synthase and, consequently, higher consumption of nicotinamide adenine dinucleotide phosphate (NADPH) through the enhanced rate of pentose-phosphate pathway activity and boosted glucose-6-phosphate 1-dehydrogenase.[37]

As the level of ROS increases, the rate of TGFβ-mediated signaling enhances the overproduction of cytokines (IL1, IL6, IL10, TNFα) and complement factors.[36,37] The accumulated ROS and reactive nitrogen species (RNS) upregulate the NF-κB pathway, which triggers NO synthase and leads to NO-mediated upregulation of prostacyclin. Unfortunately, an extremely high concentration of NO reacts with ROS and generates dangerous peroxynitrites (Fig. 2).[37,38]

Hence, our findings highlight an odd situation: On the one hand, there is excessive NO generation and, on the other hand, limited access to NO due to reacting with ROS. In turn, the overproduction of cytokines stimulates the activation of complement system elements, which were well represented in this study (Table 2).

4.3. Repressed transition from progenitor to postmitotic state

Transcriptional activation and repression of selected genes by chromatin remodeling is a crucial mechanism guiding tissue formation and organogenesis, where DPF3 plays the role of an important indicator (Table 2). Evidence suggests that the maximum expression of DPF3 is observed in the hypothalamus, neurons, myoblasts, and oocytes. Its expression is regulated through Mef2, which recognizes the DFP3 promoter with high specificity.[39] As has been seen in cultured human embryonic kidney cells and later in myoblasts, soon after switching the DFP3 gene off, the development and differentiation of cells are aborted.[40]

DFP3 orchestrates neurogenesis and myogenesis (including cardiac and skeletal muscle), but the exact mechanism of action is still uncertain. It is assumed that it acts by binding to certain acetylated and methylated regions of histones, thereby directly participating in the regulation of chromatin remodeling. Accordingly, the global estimation of the methylome has been proposed as a potential hallmark for assessing gestational diabetic conditions and its direct consequences affecting fetal development.[33] Notably, DPF3 is a necessary element of the neuron-specific chromatin remodeling complex BRG1/BRM

associated factor complex. Upon completion of the progenitor activity of neurogenic cells, the essential proliferative capacity of the neural stem/progenitor cells complex (ACTL6A/BAF53A and PHF10/BAF45A) is replaced by a neuron-specific complex comprising homologous ACTL6B/BAF53B and DPF3/BAF45C.

Some studies have shown that significantly increased DPF3 expression leads to cardiac hypertrophy during embryogenesis, while the same was also shown in adults with chronic cardiac hypertrophy.[41] On both occasions, the process of hypertrophy is associated with activation of embryo-specific genes, including the DPF3a and DPF3b isoforms, and with the reprogramming of the expression of β-MHC and skeletal actin genes. Other reports indicated that the initiation of Hirschsprung's disease is mainly due to depletion of the DFP3 gene, which causes a decrease in cell migration to the appropriate location of nerve ganglia in various parts of the intestine, especially in the stenotic segment.[42]

There is a close interaction of DPF3 with runt-related transcription factors (RUNX) signaling as part of the transforming growth factor beta (TGF-β) pathway and the increase in the proliferative rate.[43,44] The RUNX regulator leucine-rich alpha-2-glycoprotein (LRG1) is located upstream, and its increased expression is repeatedly reported in the context of various diseases due to dysregulation of the TGF-β pathway. However, in our study, increased expression of LRG1 was noted only in the CRDM group (Table 2).

Both the CRDM and CNSD groups were distinguished by DFP3, while CNSD was characterized by its lowest abundance (Table 2). Our data suggest a distinctive feature of DPF3 in association with neurons, with chromatin remodeling being executed during embryogenesis and being dramatically lower in the CNDS group. In the CRDM group, upregulation of LRG1 and DFP3 presumably reflects impaired proliferation, where DFP3 is the final point (switching to the postmitotic state) and LRG1 is the starting point, thereby determining the expression of RUNX factors and, consequently, the activity of the TGF-β pathway.

4.4. Regulation of myelinization and differentiation of cardiomyocytes via competing for canonical and noncanonical wingless-related integration site signaling pathway signaling

One of the essential participants in the organization of tissues and the process of organogenesis during embryo development proteins is LAMB4. The protein is critical for cell migration and proper orientation during organogenesis. Similar functions are performed by TSP1, which binds with PEDF, but its role is limited mainly to the adhesive tasks that determine the intercellular interaction and the interaction of cells with the extracellular space. The neurotrophic factor PEDF was found to play an active role in the genesis of neurons and cardiomyocytes (Table 2). This serine protease exhibits pronounced angiogenesis inhibition properties but does not undergo characteristic stressed/relaxed conformational changes. The highest expression of PEDF is in the retina, thalamus, dendrites, and all neurons irrespective of their topology and adaptation; the latest data also suggest expression of PEDF in liver cells.[45]

The role of PEDG in cell differentiation is to interact with extracellular matrix proteins and proteins responsible for organellar structures and cytoskeletal architecture. Among these proteins, TSP1 is the most engaging adhesive glycoprotein, which helps establish the cell-to-extracellular matrix connection and modulate CD36-mediated angiogenesis (Table 2). The pair of PEDF and TSP1 shows substantial implications in the regulation of Wnt signaling ($P = .01594$, Fig. 3).

PEDF seems to act as an endogenous inhibitor of the Wnt/β-catenin pathway through exposure to the low-density lipoprotein receptor-related protein 6 (LRP6) coreceptor. The expression level of PEDF increases significantly in response to Wnt3a, which employs LRP6 as a coreceptor for signal transmission[46] (Fig. 3). Simultaneously, it decreases in response to noncanonical Wnt5a-induced signaling, which does not go through LRP6. Compatible results were obtained using small interfering RNA when the direct interaction of PEDF with LRP6 (K_d is 3.7 nM) was abolished, promoting signal transmission via the Wnt pathway.[47] Mechanistically, abolishing ligand (Wnt3a) with receptor (LRP6) dimerization is accomplished by reducing LRP6 phosphorylation by PEDF (Fig. 3). Apparently, inhibition of canonical Wnt signaling affects downstream elements, including the suppression of TSP1 that is necessary for angiogenesis and the associated morphogenesis via TGF-β signaling. Suppression of TSP1 is manifested in a 25% decrease in 4-hydroxyproline needed for collagen synthesis and extracellular matrix structuring.

Hence, presumably, the above antagonistic relationship explains the basis of the competing experience between PEDF and TSP1 during angiogenesis. Both proteins are characterized by straight functional interactions but by inverse regulation: while the CNSD group was characterized by downregulation of PEDF and upregulation of TSP1, the opposite happened in the CRDM group, and the HPMG group was characterized by increased TSP1 (Table 2). Thus, comprehensive regulation during embryogenesis is tailored to the compensatory mechanism due to noncanonical signaling activation. This mechanism requires Wnt5a and tyrosine-protein kinase transmembrane receptor (ROR2), thereby inducing the translocation of β-catenin to the nucleus and keeping its level high enough for signal transduction.[48,49]

Considering the enhanced activity of the noncanonical Wnt pathway, we cannot ignore the extremely important DAAM2 protein that was had a frequency of detection among the population of more than 0.8 in the HPMG and CRDM groups (Table 2). DAAM2, as a switcher, governs the noncanonical Wnt pathway[50] (Fig. 4). It is an important regulator of various embryogenic processes, including the process of myelination, spinal cord development, potentiation, and clustering of signalosomes. Two isoforms exist, and both disheveled-associated activator of morphogenesis 1 and DAAM2 are necessary for the development of myocardial cells and maturation of sarcomeres through their effects on the organization of the actin cytoskeleton.[51] Disruption of DAAM2-mediated transduction leads to cerebral amyloid angiopathy, degeneration of the epithelial basement membrane, and various oncogenic manifestations.[52,53]

Noncanonical Wnt signaling cannot substitute for abolished canonical signaling. Rather, it is a cognate pathway bypassing β-catenin[54] that is necessary to control sympathetic neuron morphogenesis and the determination of cell specialization, migration, and polarization.[55–57] During the differentiation of peripheral axons from embryonic fibroblasts, Wnt5a binds to the ROR2 coreceptor, inducing the phosphorylation of DAAM2, which is a prerequisite for signal transmission[54,55] (Fig. 4).

Knockdown of Wnt5a by small interfering RNA dramatically decreased or completely abolished DAAM2 phosphorylation.[58] Other reports demonstrated that inhibition of the canonical Wnt pathway does not depend on the ROR2 coreceptor since its

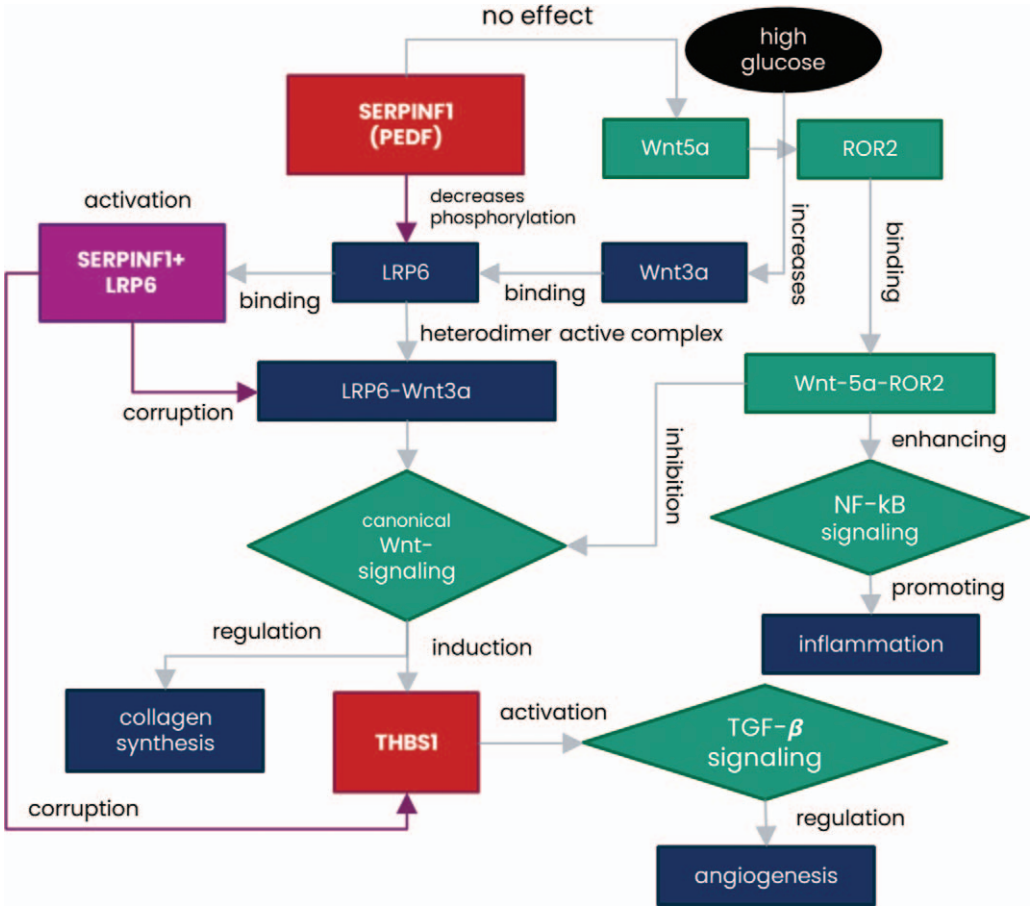

Figure 3. Regulation of Wnt signaling during embryogenesis under maternal diabetic conditions. Excessive glucose loading leads to the activation of the LRP6 coreceptor for Wnt3a. The formation of the Wnt3a-LRP6 complex is critical for activating the canonical Wnt pathway, where one of its endpoints (THBSP1) regulates the TGF-β-mediated pathway necessary to initiate angiogenesis. PEDF reduces the phosphorylation of LRP6, which contributes to competing substitution for Wnt3a by SERPINF in the binding with LRP6. At this point, the formation of the LRP6-Wnt3a complex is disrupted, which leads to inhibition of angiogenesis and related processes of matrix remodeling. Under conditions of depleted canonical Wnt signaling, the noncanonical pathway mediated by the Wnt5a and ROR2 coreceptors and resistance to the effect of PEDF is enhanced. An increasing rate of the noncanonical pathway activates NF-κB signaling, which promotes the synthesis of proinflammatory cytokines and suppresses canonical Wnt signaling.

absence or blockade retains the ability of Wnt5a and DAAM2 to switch and potentiate noncanonical signaling.[59,60]

Impaired expression of DAAM2 leads to noncompaction cardiomyopathy. At least in murine models, animals with excessive or suppressed expression of disheveled-associated activator of morphogenesis 1 or DAAM2 are characterized by the failure of nucleation of actin fibrils in embryonic fibroblasts, excessively deep trabeculae myocardial cavities, and left ventricular non-compaction cardiomyopathy (Supplemental Digital Content [Appendix C, http://links.lww.com/MD2/A650]).[61] Cardiomyocytes are round and smaller in size, with a weak interconnection, due to inhibited secretion of collagen and decreased rate of actin polymerization (Supplemental Digital Content [Appendix C, http://links.lww.com/MD2/A650]). Later, it was found that the molecular function of DAAM2 is due to the formin homology-1 domain that is necessary for the capping of actin filaments and to the formin homology-2 domain that supports the binding and assembly of actin subunits.[51] Malfunction of DAAM2 is manifested in a lack or weakly articulated *Z*-bands of sarcomeres and anatomically disorganized *M*-, *H*-, and *I*-bands,[61,62] which attracted our attention because of the extremely increased DAAM2 in the CRDM group (Table 2).

The activity of DAAM2 is involved in the regeneration of the myelin sheath of oligodendrocytes, which is inhibited after white matter injury.[63] The process is regulated via activation of the DAAM2-phosphatidylinositol 4,5-bisphosphate pathway to achieve a complex between phosphatidylinositol 4-phosphate 5-kinase and DAAM2 (Fig. 4) and to excite PLR5/6 receptors.[63,64] Here, the role of DAAM2 is restricted to the regulation of oligodendrocyte differentiation and axonal myelination, thereby increasing DAAM2 expression during embryogenesis and in adults leading to depression of myelination. In this respect, CNSD was the only group with an unaltered abundance of DAAM2 in our findings (Table 2). Experiments with DAAM2$^{-/-}$ animal embryos reported a considerably increased degree of axonal myelination and weakly controlled enhanced differentiation of oligodendrocytes.[65] Nevertheless, hypoxic conditions promote myelination, which suggests a negative effect on the DAAM2- phosphatidylinositol 4-phosphate 5-kinase axis in Wnt signaling regulation.[65]

Presumably, Wnt signaling regulation is achieved through competitive binding with LPR6 receptors, whereas binding to ROR2 receptors is necessary for interplay with DAAM2, which promotes the initiation of morphogenesis, myelination, and the

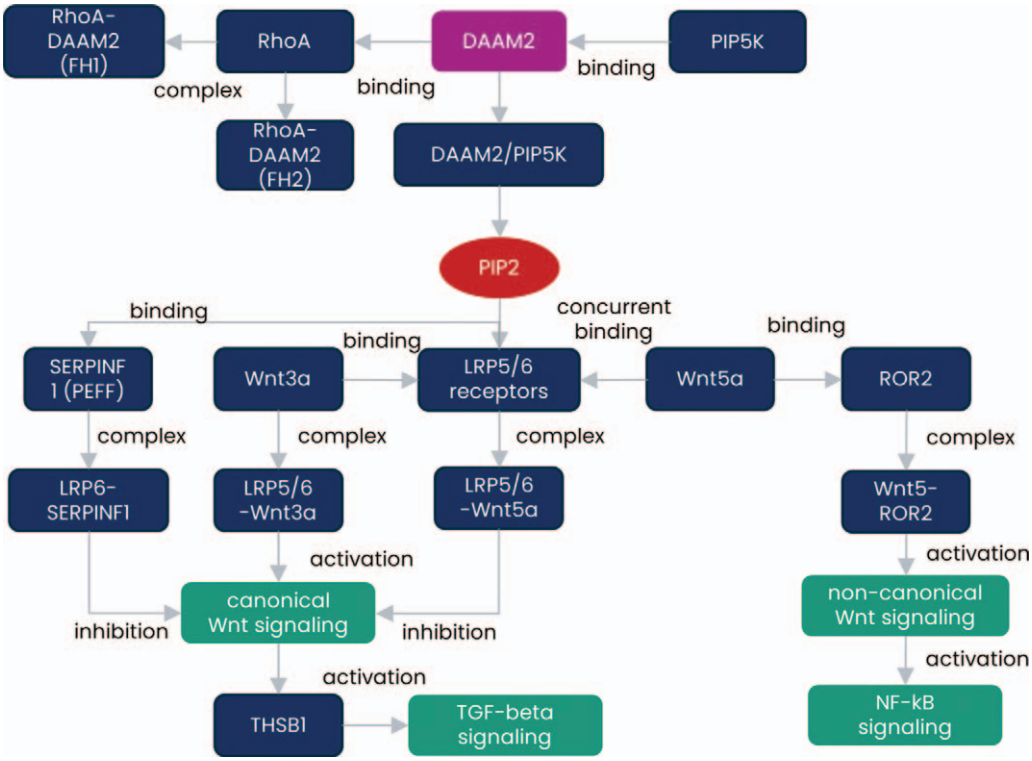

Figure 4. Proposed regulation coupled with DAAM2 activity. Formation of the DAAM2-PIP5K complex is obligatory for the phosphorylation of LPR5/6 receptors by PIP2. Activated receptors can form complexes with the Wnt3a ligand in the canonical direction or, alternatively, a competitive complex with Wnt5a, which thus inhibits canonical signal transduction and enhances the activity of the Wnt5a-ROR2-mediated pathway. Competitive inhibition of the canonical pathway can also be induced through the complexation of PEDF and LRP6 receptors that disrupts of the Wnt3-LRP6-mediated pathway. The involvement of DAAM2 in the regulation of actin polymerization and cytoskeletal arrangement is accomplished through functional complexation with the RhoA GTPase exchange factor.

immune response through potentiating NF-κB signaling (Fig. 4). Overexpression of DAAM2 during pregnancy places the developing fetus at risk of cardiomyopathy and irregular tissue development.

4.5. Coupled retinoic acid deficiency and thyroxine transport stimulate oxidative stress

Transthyretin (TTHY) is a secreted protein with an affinity for thyroxine an order of magnitude greater than for triiodothyronine, making it the primary carrier of thyroid hormone. In addition, TTHY has an extraordinary ability to transport retinoic acid (RA). It binds with 2 molecules of RBP (retinol-binding protein) in a stable complex, thereby reducing the glomerular ultrafiltration of RA and stabilizing the complex of RA with RBP.[66] Typically, up to 40% of circulating TTHY is bound with RBP, while the rest carries thyroxine (Fig. 5).

The most prevalent disease associated with TTHY is transthyretin amyloidosis, which occurs due to the inability to assemble into a regular stable homotetrameric structure and hence to transport thyroxine and RA to sites of their further transformation.[67] Clinical findings show the formation of amyloid fibrils due to the accumulation of unstructured TTHY oligomers[68] close to the ventricular septum and synaptic region of large neurons,[69] causing various types of neuropathy and cardiomyopathy.[70]

The serum concentration of TTHY in newborns varies between 50 and 200 μg/mL and rapidly increases over two-fold in adults. In patients with severe cardiomyopathy, the concentration of circulating TTHY and its fragments is approximately 250 μg/mL due to chronic transthyretin amyloidosis.[71,72] In patients with neurodegenerative diseases, its concentration and expression level are increased by an order of magnitude.[73] The acceptable range of TTHY is wide (69–650 μg/mL) and may vary in response to dietary preferences and immune response. Therefore, it is rather difficult to specify its diagnostic significance.[73,74] The expected concentration of TTHY in the blood is 200 to 400 μg/mL, and its half-life is 2 days.[71]

The abundance of TTHY directly correlates with estradiol, which increases significantly during pregnancy. Blocking estradiol or cortisol receptors is exhibited by a significant decrease in circulating TTHY.[75] According to our data, TTHY was upregulated only in the CNSD group, presumably caused by both the expected increase in estradiol and deficiency in RA (Table 2).

There are data on the latent proteolytic activity of TTHY: The protein cleaves β-amyloid into small fragments incapable of aggregating into amyloid plaques.[76] Therefore, the relationship between TTHY, lipid metabolism, and the transport of RA is important. Up to 2% of TTHY is in the complex with apolipoprotein A-I (APOA1), which exhibits antioxidant activity (Fig. 5). An increased concentration of circulating TTHY due to greater uncoupling with RBP primes its proteolytic activity, mostly focused on APOA1. Recently, the combination of substantially decreased APOA1 with higher BMI in patients with T2DM and GDM was considered a risk factor for the prediction of diabetic conditions.[77,78] Fragments of APOA1 aggregate into apolipoprotein amyloid fibrils and ultimately

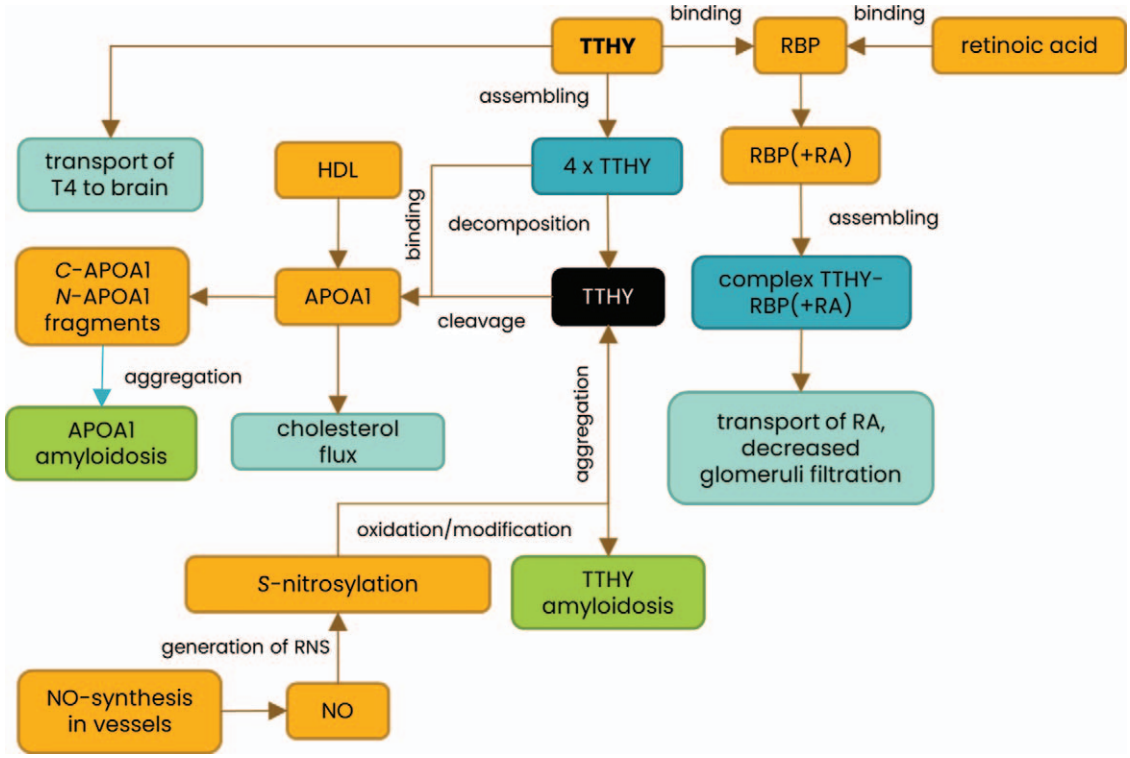

Figure 5. Normally, transthyretin (TTHY) forms functional tetramer complexes that transport thyroxin (T4) to brain cells. Up to 40% of circulating TTHY is assembled in stable complexes with RBP that binds and transports retinoic acid to reduce the glomerular filtration of retinoic acid. Up to 1% to 2% of TTHY is in complex with APOA1 in HDL particles to transfer cholesterol for deposition. While in complex, TTHY does not have lytic activity; however, unstable tetramers release a large number of free circulating TTHY subunits, which are capable of aggregating in amyloid fibrils and exhibit lytic activity toward APOA1. The affected APOA1 is cleaved into C- and N-terminal domains that form apolipoprotein fibrils. Under conditions of oxidative stress, TTHY is easily nitrolyzed by NO that is synthesized in the endothelium, thereby enhancing inactivation of TTHY and increasing the rate of its aggregation into oligomer amyloids.

cause inflammation, activation of the complement system, and augmented oxidative stress.[79]

Hence, RA deficiency can provoke undesirable consequences due to an increased concentration of circulating TTHY and consequential decline in APOA1. However, overproduction of NO in T2DM patients also accelerates oligomerization of TTHY through its *S*-nitrosylation,[80] which fosters the extension of oxidative stress (Fig. 5).

5. Conclusion

In this study, different mechanisms seemed to guide the morphogenesis that characterized different types of fetopathy, but they all emerged from the diabetic condition during pregnancy. Presumably, depending on clinical history, the strength of influence can vary, and the result can be cardiomyopathy, neuropathy, liver enlargement, or a combination of several types of fetopathy.

The defined potential serological markers are distinct from those currently utilized in clinical practice for pregnant patients with a diabetic background. The traditional characterization of these patients is based on the available tests (such as oral glucose tolerance test and homeostasis model assessment of insulin resistance) and markers (fructosamine, C-peptide, and glycated hemoglobin), detection of autoantibodies, fasting glucose level, blood glucose level after loading, etc.) or their combination. Such approaches provide essential information about the onset and progression of diabetes mellitus, but they can be ambiguous regarding diabetic fetopathy.

Most of the examined markers are participants in critical processes at different stages of embryogenesis and regulate various morphogenesis phases. There are proteins regulating mRNA splicing and DNA repair, differentiation of neurons and their switching to the postmitotic state, Wnt signaling guiding tissue morphogenesis, and the proper specialization of cardiomyocytes and oligodendrocytes. Turning to the panoply of evidence-based data, we concluded that some DNA regulating proteins (CDCL5 and PLRG1) may cause dysregulation of placental miRNAs that influence mRNA processing or splicing variants generation. These types of processes are especially profound if CNSD fetopathy is inspected. Overproduction of ROS attributed to diabetic condition provisions generalized escalation of immune response and local inflammation reaction, which are reflected in elevated levels of complement factors and TGFβ-mediated cascades, but probably such signs cannot be considered as highly specific definitely. On the other side, overexpression of DPF3 has been recently detected as a cause of cardiac hypertrophy and has been shown in the CRDM group. This can be easily coupled with impairments of neurogenesis and myelinization in combination with DAAM2 and TSP1 as the main participants of Wnt-signaling switchers. Expression of DAAM2 is capable of regulating both oligodendrocytes and cardiomyocytes differentiation but may have an opposite effect among examined types of fetopathy. Finally, retinoic acid deficiency provides an undesirable increase of circulating TTHY concentration, which affects ROS generation and APOA1 circulation, and has been monitored in all studied groups apart from the control patients.

We assume, that the present study may assist in deeper insights into the exact mechanisms leading to abnormal fetal development under maternal diabetic conditions and may suggest promising serological markers with high potency to establish signs of diabetic fetopathy at early gestational ages in comparison to the currently employed instrumental methods.

6. Limitations

The limitations of the study are mostly related to the diagnosis of fetal pathology at the current clinical state. Admittedly, the most critical issue is a limited potential for detecting and monitoring signs of diabetic fetopathy. The most robust method is sonography, but the signs can only be detected quite late (typically at week 30 of gestational age and even later). Such a late diagnosis limits the possibility of taking the appropriate corrective actions to minimize dire consequences of the maternal diabetic condition. The present study does not claim to be pioneering in the clinical diagnosis of diabetic fetopathy but rather aimed to generalize key molecular reasons for impaired fetal morphogenesis. This is a continuing and developing investigation that has evolved from the molecular features of the maternal diabetic condition during pregnancy to the detection of fetal developmental progress and pathology under the impact of maternal diabetes.

Acknowledgment

Mass spectrometric measurements were performed using the equipment of the "Human Proteome" Core Facility of the Institute of Biomedical Chemistry (Russia, Moscow).

Author contributions

Conceptualization: Sergey G. Morozov.
Data curation: Olga Papysheva, Lubov Kharitonova, Tatiana Mayatskaya, Ekaterina Schipkova, Sergey G. Morozov.
Formal analysis: Arthur T. Kopylov, Olga Papysheva, Iveta Gribova, Galina Kotaysch, Malik K. Nurbekov, Ekaterina Schipkova.
Funding acquisition: Sergey G. Morozov.
Investigation: Arthur T. Kopylov, Anna L. Kaysheva, Lubov Kharitonova.
Methodology: Arthur T. Kopylov, Iveta Gribova, Galina Kotaysch, Olga Terekhina.
Project administration: Anna L. Kaysheva, Galina Kotaysch.
Resources: Olga Papysheva, Lubov Kharitonova, Tatiana Mayatskaya.
Software: Anna L. Kaysheva, Tatiana Mayatskaya, Ekaterina Schipkova, Olga Terekhina.
Supervision: Malik K. Nurbekov.
Validation: Iveta Gribova, Malik K. Nurbekov, Olga Terekhina.
Writing – original draft: Arthur T. Kopylov, Tatiana Mayatskaya.
Writing – review & editing: Arthur T. Kopylov, Sergey G. Morozov.

References

[1] Hod M, Kapur A, Sacks DA, et al. The International Federation of Gynecology and Obstetrics (FIGO) initiative on gestational diabetes mellitus: a pragmatic guide for diagnosis, management, and care#. Int J Gynecol Obstet 2015;131:S173doi:10.1016/S0020-7292(15)30007-2.
[2] Tutino GE, Tam WH, Yang X, Chan JCN, Lao TTH, Ma RCW. Diabetes and pregnancy: perspectives from Asia. Diabet Med 2014;31:302–18.
[3] Thayer SM, Lo JO, Caughey AB. Gestational diabetes: importance of follow-up screening for the benefit of long-term health. Obstet Gynecol Clin North Am 2020;47:383–96.
[4] Durackova L, Kristufkova A, Korbel M. Pregnancy and neonatal outcomes in women with type 1 diabetes mellitus. Bratisl Lek Listy 2017;118:56–60.
[5] Boney CM, Verma A, Tucker R, Vohr BR. Metabolic syndrome in childhood: association with birth weight, maternal obesity, and gestational diabetes mellitus. Pediatrics 2005;115:e290–6.
[6] Kc K, Shakya S, Zhang H. Gestational diabetes mellitus and macrosomia: a literature review. Ann Nutr Metab 2015;66(Suppl 2):14–20.
[7] Hotamisligil GS, Peraldi P, Budavari A, Ellis R, White MF, Spiegelman BM. IRS-1-mediated inhibition of insulin receptor tyrosine kinase activity in TNF-alpha- and obesity-induced insulin resistance. Science 1996;271:665–8.
[8] Briana DD, Malamitsi-Puchner A. Reviews: adipocytokines in normal and complicated pregnancies. Reprod Sci 2009;16:921–37.
[9] Mohsin F, Khan S, Baki MA, Zabeen B, Azad K. Neonatal management of pregnancy complicated by diabetes. J Pak Med Assoc 2016;66(9 Suppl 1):S81–4.
[10] Wu Y, Liu B, Sun Y, et al. Association of maternal prepregnancy diabetes and gestational diabetes mellitus with congenital anomalies of the newborn. Diabetes Care 2020;43:2983–90.
[11] Tabib A, Shirzad N, Sheikhbahaei S, et al. Cardiac malformations in fetuses of gestational and pre gestational diabetic mothers. Iran J Pediatr 2013;23:664–8.
[12] Salbaum JM, Kappen C. Neural tube defect genes and maternal diabetes during pregnancy. Birth Defects Res A Clin Mol Teratol 2010;88:601–11.
[13] Dheen ST, Tay SSW, Boran J, et al. Recent studies on neural tube defects in embryos of diabetic pregnancy: an overview. Curr Med Chem 2009;16:2345–54.
[14] Loeken MR. Current perspectives on the causes of neural tube defects resulting from diabetic pregnancy. Am J Med Genet C Semin Med Genet 2005;135C:77–87.
[15] Alorainy IA, Barlas NB, Al-Boukai AA. Pictorial essay: infants of diabetic mothers. Indian J Radiol Imaging 2010;20:174–81.
[16] Rubarth LB. Infants of diabetic mothers. Neonatal Netw 2013;32:416–8.
[17] Hartung J, Chaoui R, Wauer R, Bollmann R. Fetal hepatosplenomegaly: an isolated sonographic sign of trisomy 21 in a case of myeloproliferative disorder. Ultrasound Obstet Gynecol Off J Int Soc Ultrasound Obstet Gynecol 1998;11:453–5.
[18] Shang M, Lin L. IADPSG criteria for diagnosing gestational diabetes mellitus and predicting adverse pregnancy outcomes. J Perinatol 2014;34:100–4.
[19] Kopylov AT, Kaysheva AL, Papysheva O, et al. Association of proteins modulating immune response and insulin clearance during gestation with antenatal complications in patients with gestational or type 2 diabetes mellitus. Cells 2020;9: doi:10.3390/cells9041032.
[20] Vaudel M, Barsnes H, Berven FS, Sickmann A, Martens L. SearchGUI: an open-source graphical user interface for simultaneous OMSSA and X! Tandem searches. Proteomics 2011;Published online doi:10.1002/pmic.201000595.
[21] Vaudel M, Burkhart JM, Zahedi RP, et al. PeptideShaker enables reanalysis of MS-derived proteomics data sets. Nat Biotechnol 2015;33:22–4.
[22] Elias JE, Gygi SP. Target-decoy search strategy for increased confidence in large-scale protein identifications by mass spectrometry. Nat Methods 2007;4:207–14.
[23] Ashburner M, Ball CA, Blake JA, et al. Gene ontology: tool for the unification of biology. The gene ontology consortium. Nat Genet 2000;25:25–9.
[24] Kanehisa M, Sato Y. KEGG Mapper for inferring cellular functions from protein sequences. Protein Sci 2020;29:28–35.
[25] Fabregat A, Jupe S, Matthews L, et al. The reactome pathway knowledgebase. Nucleic Acids Res 2018;46(D1):D649–55.
[26] Urano-Tashiro Y, Sasaki H, Sugawara-Kawasaki M, et al. Implication of Akt-dependent Prp19 alpha/14-3-3beta/Cdc5L complex formation in neuronal differentiation. J Neurosci Res 2010;88:2787–97.
[27] Tang L, Liu L, Li G, Jiang P, Wang Y, Li J. Expression profiles of long noncoding RNAs in intranasal LPS-mediated Alzheimer's disease model in mice. Biomed Res Int 2019;2019:9642589doi: 10.1155/2019/9642589.
[28] Minocha R, Popova V, Kopytova D, et al. Mud2 functions in transcription by recruiting the Prp19 and TREX complexes to transcribed genes. Nucleic Acids Res 2018;46:9749–63.

[29] Mohammad I, Nousiainen K, Bhosale SD, et al. Quantitative proteomic characterization and comparison of T helper 17 and induced regulatory T cells. PLoS Biol 2018;16:e2004194doi:10.1371/journal.pbio.2004194.
[30] Ellison EM, Bradley-Whitman MA, Lovell MA. Single-base resolution mapping of 5-hydroxymethylcytosine modifications in hippocampus of Alzheimer's disease subjects. J Mol Neurosci 2017;63:185–97.
[31] Llères D, Denegri M, Biggiogera M, Ajuh P, Lamond AI. Direct interaction between hnRNP-M and CDC5L/PLRG1 proteins affects alternative splice site choice. EMBO Rep 2010;11:445–51.
[32] Brennecke J, Stark A, Russell RB, Cohen SM. Principles of microRNA-target recognition. PLoS Biol 2005;3:e85doi:10.1371/journal.pbio.0030085.
[33] Dias S, Pheiffer C, Abrahams Y, Rheeder P, Adam S. Molecular biomarkers for gestational diabetes mellitus. Int J Mol Sci 2018;19: doi:10.3390/ijms19102926.
[34] Kleinridders A, Pogoda H-M, Irlenbusch S, et al. PLRG1 is an essential regulator of cell proliferation and apoptosis during vertebrate development and tissue homeostasis. Mol Cell Biol 2009;29:3173–85.
[35] Fortschegger K, Wagner B, Voglauer R, Katinger H, Sibilia M, Grillari J. Early embryonic lethality of mice lacking the essential protein SNEV. Mol Cell Biol 2007;27:3123–30.
[36] Wright EJ, Scism-Bacon JL, Glass LC. Oxidative stress in type 2 diabetes: the role of fasting and postprandial glycaemia. Int J Clin Pract 2006;60:308–14.
[37] Santilli F, Cipollone F, Mezzetti A, Chiarelli F. The role of nitric oxide in the development of diabetic angiopathy. Horm Metab Res 2004;36:319–35.
[38] Akiibinu MO, Ogundahunsi OA, Ogunyemi EO. Inter-relationship of plasma markers of oxidative stress and thyroid hormones in schizophrenics. BMC Res Notes 2012;5:169doi: 10.1186/1756-0500-5-169.
[39] Lange M, Kaynak B, Forster UB, et al. Regulation of muscle development by DPF3, a novel histone acetylation and methylation reader of the BAF chromatin remodeling complex. Genes Dev 2008;22:2370–84.
[40] Hoyal CR, Kammerer S, Roth RB, et al. Genetic polymorphisms in DPF3 associated with risk of breast cancer and lymph node metastases. J Carcinog 2005;4:13doi: 10.1186/1477-3163-4-13.
[41] Cui H, Schlesinger J, Schoenhals S, et al. Phosphorylation of the chromatin remodeling factor DPF3a induces cardiac hypertrophy through releasing HEY repressors from DNA. Nucleic Acids Res 2016;44:2538–53.
[42] Liu H, Luo Y, Li S, Wang S, Wang N, Jin X. Expression profiles of HA117 and its neighboring gene DPF3 in different colon segments of Hirschsprung's disease. Int J Clin Exp Pathol 2014;7:3966–74.
[43] Zhou Y, Zhang X, Zhang J, Fang J, Ge Z, Li X. LRG1 promotes proliferation and inhibits apoptosis in colorectal cancer cells via RUNX1 activation. PLoS One 2017;12:e0175122doi:10.1371/journal.pone.0175122.
[44] Zhang X, Xiao Z, Liu X, et al. The potential role of ORM2 in the development of colorectal cancer. PLoS One 2012;7:e31868doi:10.1371/journal.pone.0031868.
[45] Uhlén M, Fagerberg L, Hallström BM, et al. Proteomics. Tissue-based map of the human proteome. Science 2015;347:1260419doi: 10.1126/science.1260419.
[46] Protiva P, Gong J, Sreekumar B, et al. Pigment Epithelium-Derived Factor (PEDF) Inhibits Wnt/(-catenin Signaling in the Liver. Cell Mol Gastroenterol Hepatol 2015;1:535–49.
[47] Park K, Lee K, Zhang B, et al. Identification of a novel inhibitor of the canonical Wnt pathway. Mol Cell Biol 2011;31:3038–51.
[48] Xin H, Xin F, Zhou S, Guan S. The Wnt5a/Ror2 pathway is associated with determination of the differentiation fate of bone marrow mesenchymal stem cells in vascular calcification. Int J Mol Med 2013;31:583–8.
[49] Yuan Y, Niu CC, Deng G, et al. The Wnt5a/Ror2 noncanonical signaling pathway inhibits canonical Wnt signaling in K562 cells. Int J Mol Med 2011;27:63–9.
[50] Saito-Diaz K, Chen TW, Wang X, et al. The way Wnt works: components and mechanism. Growth Factors 2013;31:1–31.
[51] Habas R, Kato Y, He X. Wnt/Frizzled activation of Rho regulates vertebrate gastrulation and requires a novel Formin homology protein Daam1. Cell 2001;107:843–54.
[52] Katoh M, Katoh M. Identification and characterization of human DAAM2 gene in silico. Int J Oncol 2003;22:915–20.
[53] Yang T-L, Shen H, Liu A, et al. A road map for understanding molecular and genetic determinants of osteoporosis. Nat Rev Endocrinol 2020;16:91–103.
[54] Mikels AJ, Nusse R. Purified Wnt5a protein activates or inhibits beta-catenin-TCF signaling depending on receptor context. PLoS Biol 2006;4: e115doi:10.1371/journal.pbio.0040115.
[55] Veeman MT, Axelrod JD, Moon RT. A second canon. Functions and mechanisms of beta-catenin-independent Wnt signaling. Dev Cell 2003;5:367–77.
[56] Angers S, Moon RT. Proximal events in Wnt signal transduction. Nat Rev Mol Cell Biol 2009;10:468–77.
[57] Ho H-YH , Susman MW, Bikoff JB, et al. Wnt5a-Ror-Dishevelled signaling constitutes a core developmental pathway that controls tissue morphogenesis. Proc Natl Acad Sci U S A 2012;109:4044–51.
[58] Schlessinger K, McManus EJ, Hall A. Cdc42 and noncanonical Wnt signal transduction pathways cooperate to promote cell polarity. J Cell Biol 2007;178:355–61.
[59] Grumolato L, Liu G, Mong P, et al. Canonical and noncanonical Wnts use a common mechanism to activate completely unrelated coreceptors. Genes Dev 2010;24:2517–30.
[60] Katoh M, Katoh M. Transcriptional mechanisms of WNT5A based on NF-kappaB, Hedgehog, TGFbeta, and Notch signaling cascades. Int J Mol Med 2009;23:763–9.
[61] Ajima R, Bisson JA, Helt J-C, et al. DAAM1 and DAAM2 are co-required for myocardial maturation and sarcomere assembly. Dev Biol 2015;408:126–39.
[62] Mezzano V, Pellman J, Sheikh F. Cell junctions in the specialized conduction system of the heart. Cell Commun Adhes 2014;21:149–59.
[63] Lee HK, Chaboub LS, Zhu W, et al. Daam2-PIP5K is a regulatory pathway for Wnt signaling and therapeutic target for remyelination in the CNS. Neuron 2015;85:1227–43.
[64] Pan W, Choi S-C, Wang H, et al. Wnt3a-mediated formation of phosphatidylinositol 4,5-bisphosphate regulates LRP6 phosphorylation. Science 2008;321:1350–3.
[65] van den Bout I, Divecha N. PIP5K-driven PtdIns(4,5)P2 synthesis: regulation and cellular functions. J Cell Sci 2009;122(Pt 21):3837–50.
[66] Getz RK, Kennedy BG, Mangini NJ. Transthyretin localization in cultured and native human retinal pigment epithelium. Exp Eye Res 1999;68:629–36.
[67] González-López E, López-Sainz Á, Garcia-Pavia P. Diagnosis and treatment of transthyretin cardiac amyloidosis. Progress and Hope. Rev Esp Cardiol (Engl Ed) 2017;70:991–1004.
[68] Galant NJ, Westermark P, Higaki JN, Chakrabartty A. Transthyretin amyloidosis: an under-recognized neuropathy and cardiomyopathy. Clin Sci (Lond) 2017;131:395–409.
[69] Sekijima Y, Transthyretin . (ATTR) amyloidosis: clinical spectrum, molecular pathogenesis and disease-modifying treatments. J Neurol Neurosurg Psychiatry 2015;86:1036–43. doi: 10.1136/jnnp-2014-308724.
[70] Maurer MS, Elliott P, Comenzo R, Semigran M, Rapezzi C. Addressing common questions encountered in the diagnosis and management of cardiac amyloidosis. Circulation 2017;135:1357–77.
[71] Buxbaum J, Koziol J, Connors LH. Serum transthyretin levels in senile systemic amyloidosis: effects of age, gender and ethnicity. Amyloid Int J Exp Clin Investig Off J Int Soc Amyloidosis 2008;15:255–61.
[72] Hanson JLS, Arvanitis M, Koch CM, et al. Use of serum transthyretin as a prognostic indicator and predictor of outcome in cardiac amyloid disease associated with wild-type transthyretin. Circ Heart Fail 2018;11: e004000doi:10.1161/CIRCHEARTFAILURE.117.004000.
[73] Soprano DR, Herbert J, Soprano KJ, Schon EA, Goodman DS. Demonstration of transthyretin mRNA in the brain and other extrahepatic tissues in the rat. J Biol Chem 1985;260:11793–8.
[74] Li X, Masliah E, Reixach N, Buxbaum JN. Neuronal production of transthyretin in human and murine Alzheimer's disease: is it protective? J Neurosci 2011;31:12483–90.
[75] Martinho A, Gonçalves I, Costa M, Santos CR. Stress and glucocorticoids increase transthyretin expression in rat choroid plexus via mineralocorticoid and glucocorticoid receptors. J Mol Neurosci 2012;48:1–13.
[76] Silva CS, Eira J, Ribeiro CA, et al. Transthyretin neuroprotection in Alzheimer's disease is dependent on proteolysis. Neurobiol Aging 2017;59:10–4.
[77] Wu X, Yu Z, Su W, et al. Low levels of ApoA1 improve risk prediction of type 2 diabetes mellitus. J Clin Lipidol 2017;11:362–8.
[78] Dullaart RPF, Pagano S, Perton FG, Vuilleumier N. Antibodies against the C-terminus of ApoA-1 are inversely associated with cholesterol efflux capacity and HDL metabolism in subjects with and without type 2 diabetes mellitus. Int J Mol Sci 2019;20: doi:10.3390/ijms20030732.
[79] Sharma M, Khan S, Rahman S, Singh LR. The extracellular protein. Transthyretin is an oxidative stress biomarker. Front Physiol 2019;10:5doi: 10.3389/fphys.2019.00005.
[80] Saito S, Ando Y, Nakamura M, et al. Effect of nitric oxide in amyloid fibril formation on transthyretin-related amyloidosis. Biochemistry 2005;44:11122–9.